Journal of Physiology (2002), **544.1**, *pp.* 253–265
DOI: 10.1113/jphysiol.2002.019687

www.jphysiol.org

Journal of Physiology

Role of synaptic inhibition in turtle respiratory rhythm generation

Stephen M. Johnson *, Julia E. R. Wilkerson * †, Michael R. Wenninger *, Daniel R. Henderson * and Gordon S. Mitchell *

* *Department of Comparative Biosciences, School of Veterinary Medicine and* † *Neuroscience Training Program, University of Wisconsin, Madison, WI 53706, USA*

In vitro **brainstem and brainstem–spinal cord preparations were used to determine the role of synaptic inhibition in respiratory rhythm generation in adult turtles. Bath application of bicuculline (a $GABA_A$ receptor antagonist) to brainstems increased hypoglossal burst frequency and amplitude, with peak discharge shifted towards the burst onset. Strychnine (a glycine receptor antagonist) increased amplitude and frequency, and decreased burst duration, but only at relatively high concentrations (10–100 μM). Rhythmic activity persisted during combined bicuculline and strychnine application (50 μM each) with increased amplitude and frequency, decreased burst duration, and a rapid onset–decrementing burst pattern. The bicuculline–strychnine rhythm frequency decreased during μ-opioid receptor activation or decreased bath P_{CO_2}. Synaptic inhibition blockade in the brainstem of brainstem–spinal cord preparations increased burst amplitude in spinal expiratory (pectoralis) nerves and nearly abolished spinal inspiratory activity (serratus nerves), suggesting that medullary expiratory motoneurons were mainly active. Under conditions of synaptic inhibition blockade *in vitro*, the turtle respiratory network was able to produce a rhythm that was sensitive to characteristic respiratory stimuli, perhaps via an expiratory (rather than inspiratory) pacemaker-driven mechanism. Thus, these data indicate that the adult turtle respiratory rhythm generator has the potential to operate in a pacemaker-driven manner.**

(Received 28 February 2002; accepted after revision 15 July 2002; first published online 9 August 2002)
Corresponding author S. M. Johnson: Department of Comparative Biosciences, School of Veterinary Medicine, University of Wisconsin, 2015 Linden Drive, Madison, WI 53706, USA. Email: johnsons@svm.vetmed.wisc.edu

Most vertebrate rhythmic motor networks require synaptic inhibition to regulate timing and pattern. For example, network models of respiratory rhythm generation generally include groups of neurons that are reciprocally coupled via inhibitory synaptic connections, thereby establishing exclusive bursts of activity associated with the phases of respiration (reviewed in Richter *et al.* 1992, 1997; Duffin *et al.* 1995; Ramirez & Richter, 1996; Rybak *et al.* 1997; Richter & Spyer, 2001). Other models of respiratory rhythm generation propose that pacemaker neurons contribute to the basic respiratory rhythm without the need for synaptic inhibition (Feldman & Cleland, 1982; Getting, 1988). Evidence for potential involvement of pacemaker neurons in respiratory rhythm generation includes: (1) persistent rhythmic inspiratory activity during blockade of inhibitory synaptic transmission with $GABA_A$ and glycine antagonists, or removal of extracellular chloride ions in tadpole brainstems *in vitro* (Galante *et al.* 1996) and neonatal rat preparations *in vitro* (Smith & Feldman 1987; Feldman *et al.* 1989, 1990; Shao & Feldman, 1997; Brockhaus & Ballanyi, 1998; Bou-Flores & Berger, 2001; Johnson *et al.* 2001*a*), and (2) demonstration of conditional pacemaker neurons in the pre-Bötzinger complex (Smith *et al.* 1991; Johnson *et al.* 1994; Rekling *et al.* 1996; Koshiya & Smith, 1999; Thoby-Brisson & Ramirez, 2000, 2001), a region necessary for normal respiratory activity in anaesthetized cats (Ramirez *et al.* 1998) and awake rats (Gray *et al.* 2001). The hybrid pacemaker–network model hypothesizes that pacemaker neurons embedded within a network of excitatory and inhibitory synaptic interactions play an important role in respiratory rhythm production (Smith *et al.* 1991; Funk & Feldman, 1995; Rekling & Feldman, 1998; Butera *et al.* 1999*a*, *b*; Koshiya & Smith, 1999; Smith *et al.* 2000). Likewise, in the group pacemaker model, inspiratory bursts are an emergent property of special neurons with pacemaker properties that are mutually interconnected by excitatory synapses (Rekling & Feldman, 1998; Del Negro *et al.* 2002).

To reconcile network *vs.* pacemaker-driven models, pacemaker neurons were hypothesized to be important in neonates and young animals, but synaptic inhibition was thought to become increasingly important during maturation (Hayashi & Lipski, 1992; Duffin *et al.* 1995; Paton *et al.* 1994; Paton & Richter, 1995; Galante *et al.* 1996; Ramirez *et al.* 1996; Richter & Spyer, 2001). This hypothesis is controversial because rhythmic respiratory activity persists during synaptic inhibition blockade in

medullary slices from day 22 postnatal mice (Ramirez *et al.* 1996), 7 days after the proposed transformation from a pacemaker-driven to a network-driven system (see discussion in Funk & Feldman, 1995). Alternatively, the 'switching' hypothesis suggests that respiration is switched from a network-based system to a pacemaker-driven system under conditions of decreased synaptic inhibition and increased extracellular [K^+], thereby permitting pacemaker neurons that are not normally part of the rhythm generator to burst, forcing respiratory neurons to oscillate rhythmically (Rybak *et al.* 2001; see also Büsselberg *et al.* 2001).

Our goal was to determine whether respiratory rhythm persists during synaptic inhibition blockade using recently developed *in vitro* adult turtle preparations, and to determine if the persistent rhythm is respiratory-related. Turtle brainstem (–spinal cord) preparations are fully mature, remain viable under *in vitro* conditions for > 6 h at temperatures physiologically appropriate for turtles, and produce patterns of expiratory and inspiratory activity similar to intact turtles (Douse & Mitchell, 1990; Johnson *et al.* 1998; Johnson & Mitchell, 1998). This is the first report describing the effects of combined $GABA_A$ and glycine receptor blockade on respiratory activity in an adult poikilothermic vertebrate under *in vitro* conditions. Such information is necessary for a full understanding of the biological significance of synaptic inhibition in respiratory motor control. A preliminary report has been published in abstract form (Johnson *et al.* 2001*b*).

METHODS

All experiments were approved by the Animal Care and Use Committee at the University of Wisconsin-Madison School of Veterinary Medicine. Adult red-eared slider turtles (*Trachemys*, $n = 78, 705 \pm 13$ g) were obtained from commercial suppliers and kept in large open tanks where they had access to water for swimming, and heat lamps and dry areas for basking. Room temperature was 27–28 °C with light 14 h per day. Turtles were fed ReptoMin floating food sticks (Tetra, Blacksburg, VA, USA) 3–4 times per week.

Turtle brainstem and brainstem–spinal cord preparations

The isolation of the brainstem or brainstem–spinal cord has been described previously (Johnson *et al.* 1998; Johnson & Mitchell, 1998). Briefly, turtles were intubated and anaesthetized with 4 % halothane or isoflurane in 100 % O_2 until the limb withdrawal reflex to noxious foot pinch was eliminated. All turtles were decerebrated, rendering them insentient to pain. Anaesthetic was subsequently withdrawn. The brainstem or brainstem and spinal cord were removed and pinned down on Sylgard in a recording chamber. The tissue was superfused (4–6 ml min^{-1}) with a solution containing Hepes (*N*-[2-hydroxyethyl]piperazine-*N*′-[2-ethane-sulfonic acid]) buffer as follows (mM): 100 NaCl, 23 $NaHCO_3$, 10 glucose, 5 Hepes (sodium salt), 5 Hepes (free acid), 2.5 $CaCl_2$, 2.5 $MgCl_2$, 1.0 K_2PO_4, and 1.0 KCl. The Hepes solution was bubbled with 5 % CO_2–95 % O_2 to maintain a pH of ~7.4, as measured periodically with a calomel glass pH electrode (Digi-Sense, Cole-Parmer Instrument Co., Vernon Hills, IL, USA). In experiments using brainstem–spinal cord preparations, plastic barriers sealed with petroleum jelly were used to partition the bath into three compartments in order to apply drugs to the brainstem only (see Fig. 8 in Johnson & Mitchell, 1998). All drugs and chemicals were obtained from Sigma/RBI Aldrich (St Louis, MO, USA). All preparations were allowed to equilibrate for 4–5 h before initiating a protocol.

Electrophysiological recordings

To record bursts of respiratory motor activity, glass suction electrodes were attached to hypoglossal nerve rootlets in brainstem preparations (Fig. 1) or hypoglossal, pectoralis (expiratory), and serratus (inspiratory) nerves in brainstem–spinal cord preparations (see Fig. 8 in Johnson & Mitchell, 1998). Signals were amplified (× 10 000) and band-pass filtered (10–10 000 Hz) using a differential AC amplifier (model 1700, A-M Systems, Everett, WA, USA) before being rectified and integrated (time constant = 200 ms) using a moving averager (MA-821/RSP, CWE, Inc., Ardmore, PA, USA). The signals were then digitized and analysed using Axoscope software (Axon Instruments, Union City, CA, USA).

Experimental protocols

For dose–response curves, integrated hypoglossal bursts were recorded for 30 min (baseline) before switching to a superfusate containing drugs at progressively increasing concentrations (every 45 min). The drugs tested included: strychnine (a glycine receptor antagonist), bicuculline (a $GABA_A$ receptor antagonist), 2-hydroxysaclofen (a $GABA_B$ receptor antagonist), or DAMGO ([D-Ala^2,*N*-Me-Phe^4,Gly^5-ol] enkephalin; a μ-opioid agonist). Bursts recorded during the last 20 min of drug application were analysed. After the last drug application, brainstems were bathed with drug-free standard solution for 90–120 min to obtain washout data. In other experiments, baseline data were recorded for 30 min before switching to solution containing both bicuculline and strychnine (50 μM each; pH ~7.4). After allowing 2.5 h for the rhythm to stabilize, the superfusate was switched to either bicuculline–strychnine solution with a lower P_{CO_2} (bubbled

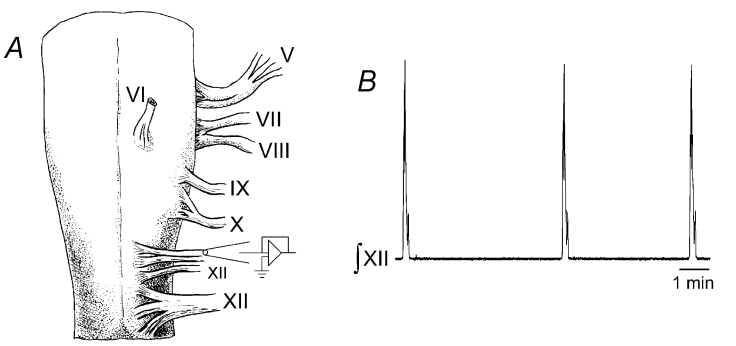

Figure 1. Spontaneous respiratory motor activity produced by *in vitro* turtle brainstem preparations

A, turtle brainstems were isolated, placed in an *in vitro* recording chamber, and suction electrodes were attached to hypoglossal (XII) nerve rootlets to record respiratory activity. *B*, a sample recording trace shows rhythmic bursts of integrated respiratory activity.

with 1.1–1.2 % CO_2 in O_2), or bicuculline–strychnine solution containing DAMGO. After a 60 min application, washout data were obtained by bathing brainstems in bicuculline–strychnine solution at pH ~7.4. For brainstem–spinal cord preparations, baseline data were recorded for 30 min before bathing the brainstem compartment with bicuculline–strychnine solution (50 μM each).

Data analysis and statistics

Respiratory burst variables were measured as described previously (Johnson *et al.* 1998; Johnson & Mitchell, 1998). Amplitude was measured at the highest point of integrated discharge trajectory in arbitrary units, and normalized to the average amplitude recorded during the baseline period. Two or more bursts separated by less than the average duration of a single burst were defined as an episode; only the first burst of an episode was measured for amplitude data (Johnson & Mitchell, 1998). Frequency was calculated as the number of bursts per 10 min, while burst duration was measured from burst onset to burst termination. Peak time was calculated by dividing the time to peak by burst duration to determine the relative timing of the peak during bursts (reported as a percentage). All measurements were averaged into bins and reported as means ± S.E.M. For statistical inferences, a one-way ANOVA with repeated measures design (Sigma Stat, Jandel Scientific Software, San Rafael, CA, USA) was used to determine if data were different from the baseline period. Individual, *post hoc* comparisons were made using Dunnett's test. *P* values < 0.05 were considered significant.

RESULTS

Blockade of glycine receptors

Strychnine application to brainstems (n = 13) elicited dose-dependent changes in respiratory burst amplitude, frequency and duration without causing erratic or tonic activity (Fig. 2*A*). Amplitude was not altered at 0.01–1.0 μM, but increased slightly at 10 μM, and increased by 110 % at 50 μM ($P < 0.05$; Fig. 2*B*). Frequency tended to increase between 0.01 and 1.0 μM, and increased by 145–155 % at 10–50 μM ($P < 0.05$; Fig. 2*C*). Burst duration decreased by 30–50 % in a dose-dependent manner at 1.0–50 μM (Fig. 2*D*). Although strychnine appeared to alter the hypoglossal burst pattern from an incrementing–decrementing pattern to a rapid onset–decrementing pattern (e.g. Fig. 2*A*), peak time was not significantly altered (Fig. 2*E*). Strychnine-

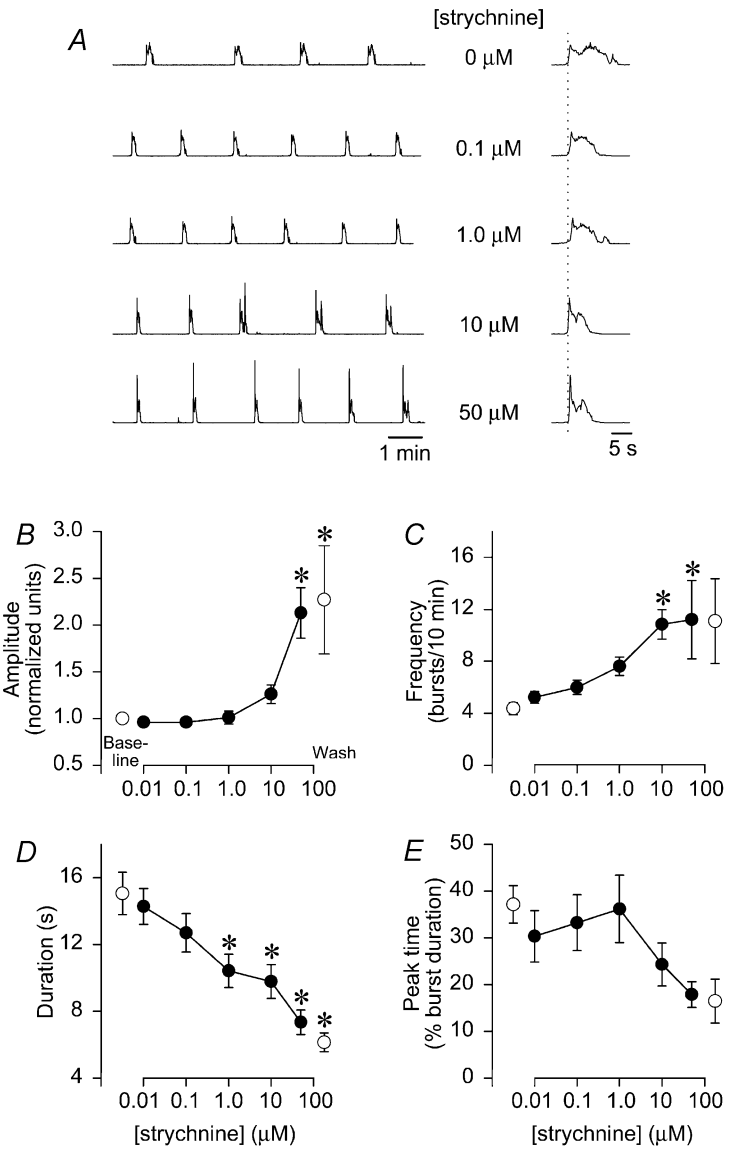

Figure 2. Glycine receptor blockade alters hypoglossal burst amplitude, frequency, and duration

A, integrated hypoglossal bursts are shown following glycine receptor blockade with increasing strychnine concentrations (0–50 μM). Individual bursts shown on a faster time scale are aligned to the onset of hypoglossal burst onset (vertical dotted line; right-hand side). *B*–*E*: ●, group data during drug application; ○, group baseline data (left) and washout data (right) in each graph. *B*, amplitude was not significantly altered until the strychnine concentration reached 50 μM. *C*, frequency tended to increase between 0.01–1.0 μM, and increased by > 100 % at 10–50 μM. *D*, duration decreased by 30–50 % at 1.0–50 μM. *E*, peak time was not significantly altered, although there was a tendency for a shift to a rapid onset–decrementing pattern at 10–50 μM. No strychnine effects were reversed during washout. * $P < 0.05$ relative to baseline. All data were derived from 13 brainstems except for the 50 μM (n = 7) and washout data (n = 4).

dependent changes in amplitude, frequency and duration were not reversed after a 90 min washout ($n = 4/13$ preparations).

Blockade of $GABA_A$ and $GABA_B$ receptors

Bicuculline application to brainstems ($n = 11$) produced complex changes in integrated hypoglossal respiratory output (Fig. 3*A*). At 0.1–1.0 μM bicuculline, hypoglossal amplitude, frequency and duration were unaltered (Fig 3*B–D*), with a tendency for a rapid onset–decrementing pattern (Fig. 3*E*). At 10 μM, hypoglossal activity was erratic with highly variable bursts (Fig. 3*A*). Frequency increased by 10 ± 1.0 bursts (10 min)$^{-1}$ ($P < 0.05$; Fig. 3*C*) and there was a shift to a rapid onset–decrementing pattern with a peak time of 13 ± 2 % ($P < 0.05$; Fig. 3*E*). At 50 μM, regular rhythmic bursts were observed (Fig. 3*A*) with amplitude increased by 130 ± 4 % ($P < 0.05$; Fig. 3*B*), frequency increased by 3.4 ± 0.7 bursts (10 min)$^{-1}$ ($P < 0.05$; Fig. 3*C*), and peak time decreased to 10 ± 1 % ($P < 0.05$; Fig. 2*E*). Burst duration was not altered by 0.1–50 μM bicuculline. Application of a $GABA_B$ receptor antagonist (2-hydroxysaclofen, 0.01–50 μM) to brainstems ($n = 8$) did not alter amplitude, frequency, duration or peak time (Fig. 4*A–D*).

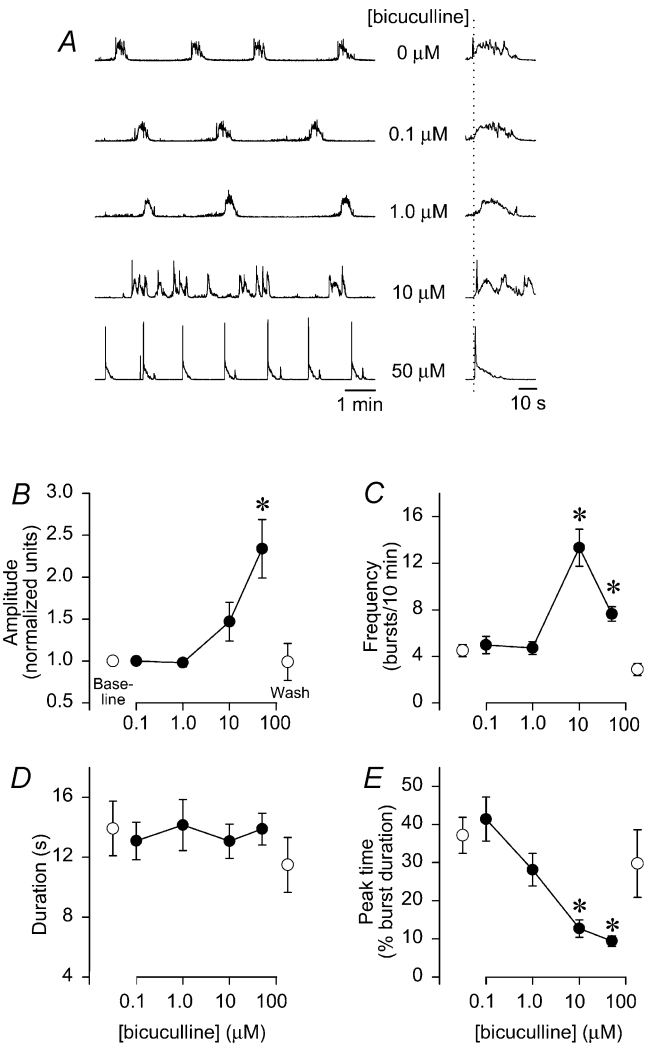

Figure 3. $GABA_A$ receptor blockade alters burst amplitude, frequency, and pattern

A, traces of integrated hypoglossal respiratory motor output are shown with increasing bicuculline concentrations (0–50 μM). *B–E*, group data from 11 brainstems are shown with the same symbols as in Fig. 2. *B*, bicuculline tended to increase amplitude at 10 μM, and significantly increased amplitude by > 200 % at 50 μM. *C*, frequency was significantly increased at 10 and 50 μM by 4–8 bursts (10 min)$^{-1}$. *D*, burst duration was unaltered at all bicuculline concentrations, but there was a dose-dependent decrease in peak time ($P < 0.05$ at 10 and 50 μM), reflecting a shift to a rapid onset–decrementing pattern. *E*, all bicuculline effects were reversible following washout ($n = 4$).

Rhythmic activity persists following combined $GABA_A$ and glycine receptor blockade

To test whether rhythmic activity persisted during combined synaptic inhibition blockade, bicuculline and strychnine (50 μM each) were applied simultaneously to brainstems ($n = 11$). Shortly after drug application, frequency increased, bursts were superimposed on tonic activity and then a high-frequency rhythm emerged with large amplitude bursts in a rapid onset–decrementing pattern (Figs. 5*A* and *B*). During combined blockade, amplitude increased by 180 ± 50 % ($P < 0.05$; Fig. 5*C*), frequency increased by 6.3 ± 1.3 bursts (10 min)$^{-1}$ ($P < 0.05$; Fig. 5*D*), duration decreased by ~22 % ($P < 0.05$; Fig. 5*E*) and peak time decreased from 36 % to 11 % ($P < 0.05$; Fig. 5*F*). The persistent rhythm produced during $GABA_A$ and glycine receptor blockade is hereafter referred to as the bicuculline–strychnine rhythm. Washout was not attempted since strychnine effects were not reversible (see Fig. 2).

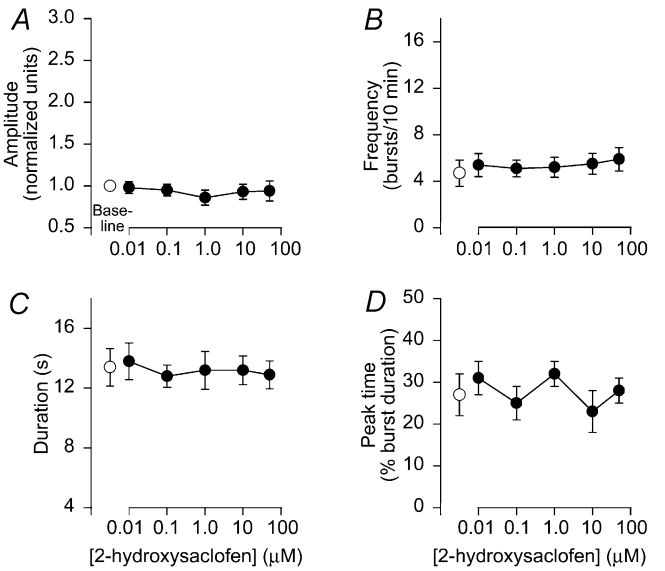

Figure 4. $GABA_B$ receptor blockade had no effect on respiratory activity

$GABA_B$ receptor blockade with increasing concentrations of 2-hydroxysaclofen did not alter burst amplitude (*A*), frequency (*B*), duration (*C*), or peak time (*D*). Symbols as in Fig. 2.

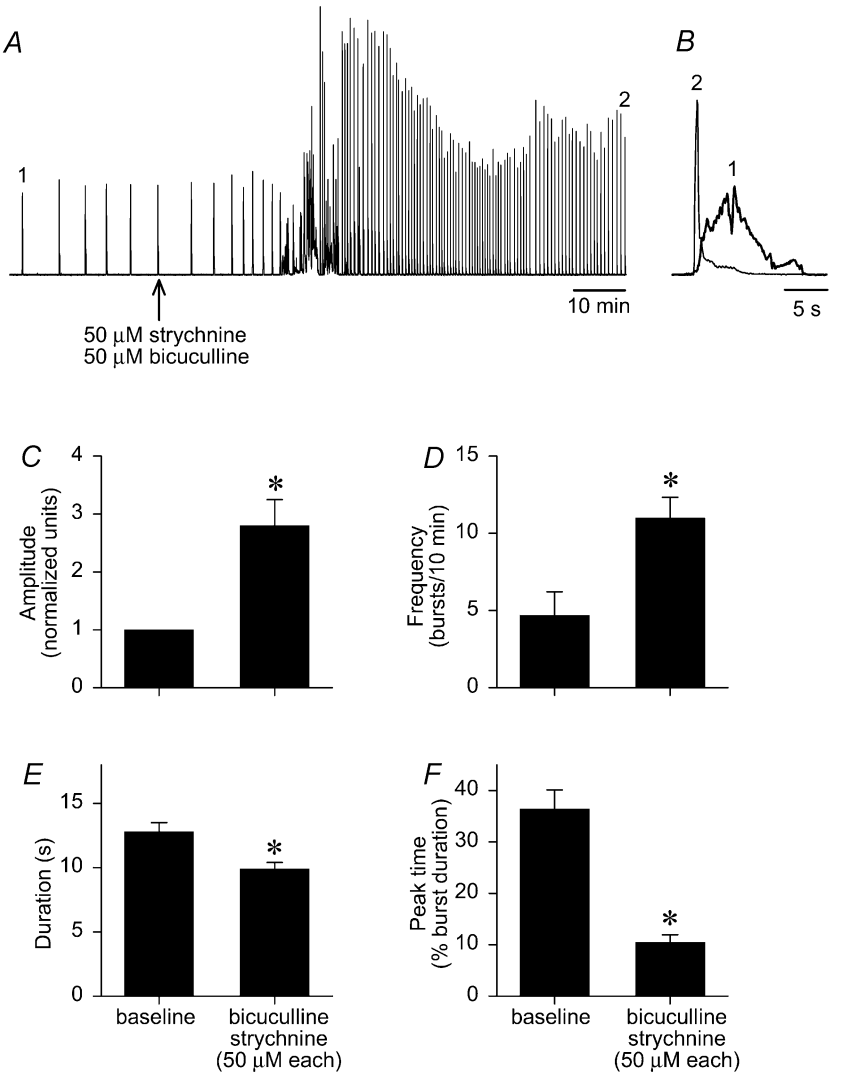

Figure 5. Rhythmic activity persists during combined $GABA_A$ and glycine receptor blockade

Bicuculline and strychnine (50 μM each) were applied to brainstems (n = 11) to block $GABA_A$ and glycine receptors, respectively. *A*, a trace of integrated hypoglossal bursts from one brainstem shows that $GABA_A$ and glycine receptor blockade caused an initial increase in frequency, followed by bursts superimposed on tonic activity. Afterwards, a high frequency rhythm emerged with large amplitude bursts. *B*, a comparison of a hypoglossal burst trace during baseline (1, thick line trace) with a hypoglossal burst trace after blocking $GABA_A$ and glycine receptors (2, thin line trace) shows the shift to rapid onset–decrementing pattern of discharge. Group data show that amplitude (*C*) and frequency (*D*) increased significantly by > 100 % while duration (*E*) and peak time (*F*) decreased significantly. Data gathered over 30 min were averaged to give baseline; blockade value is the average of data gathered over 20 min.

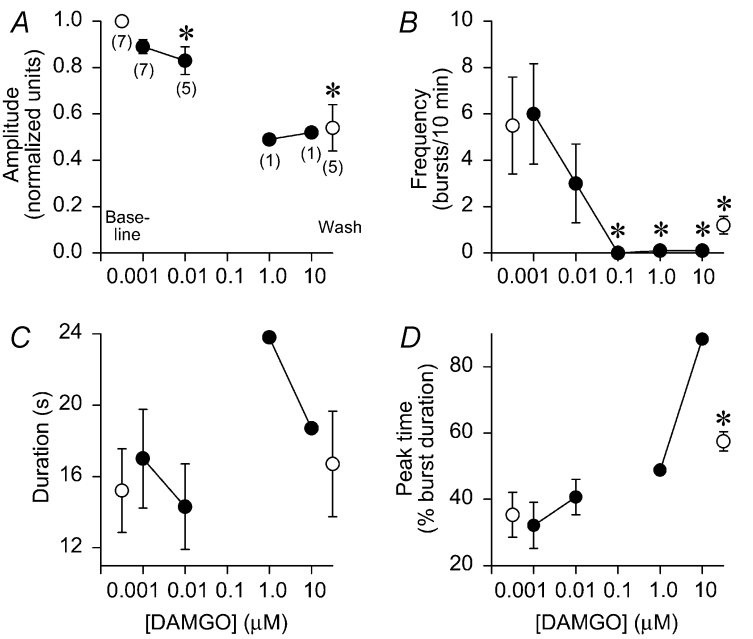

Figure 6. Activation of μ-opioid receptors abolishes respiratory activity

Application of DAMGO (a μ-opioid receptor agonist) had no effect at 0.001 μM, but decreased respiratory burst amplitude and frequency at 0.01–10 μM. *A*, amplitude was significantly decreased by 17 % at 0.01 μM and was decreased by ~50 % at 1.0 and 10 μM (insufficient data available for statistical analysis), and following washout. Numbers in parentheses below symbols indicate the number of brainstems producing respiratory activity; otherwise the symbols are as in Fig. 2. *B*, frequency decreased at 0.01 μM and was abolished in 7/7 brainstems at 0.1 μM ($P < 0.05$), and 6/7 brainstems at 1.0 and 10 μM ($P < 0.05$). There were no significant changes in burst duration (*C*) or peak time (*D*).

Bicuculline–strychnine rhythm altered by μ-opioid receptor activation and CO_2/pH changes

To test whether the bicuculline–strychnine rhythm could be altered by characteristic respiratory stimuli, such as μ-opioid receptor activation and CO_2/pH changes, control experiments were performed to examine time-dependent changes in bicuculline–strychnine rhythm frequency. Bicuculline and strychnine (50 μM each) were applied to brainstems ($n = 12$) for 5 h. Within 45–60 min of drug application, a steady-state bicuculline–strychnine rhythm was established with a frequency of 17 ± 2 bursts (10 min)$^{-1}$. The frequency then remained within 17.4–18.5 bursts (10 min)$^{-1}$ for the next 80 min (● in Fig. 7*C* and *D*). Amplitude was unaltered during this 100 min period; bursts were only 1 ± 3 % larger at the end compared to the beginning of the 100 min period. Consequently, experimental protocols on the bicuculline–strychnine rhythm were performed after bicuculline and strychnine had been applied for 1.5–2.0 h.

Opiate receptor activation. DAMGO (a μ-opioid agonist) was applied at increasing concentrations to determine which concentration abolished respiratory activity in brainstems ($n = 7$) bathed in control superfusate (Fig. 6). At 0.001–0.01 μM, DAMGO had little effect, but activity was abolished in six of seven brainstems at 0.1–10 μM ($P < 0.05$; Fig. 6*B*). Amplitude decreased by 17 % at 0.01 μM ($P < 0.05$) and was decreased at 1.0–10 μM, but statistics were not calculated because $n = 1$ (Fig. 6*A*). Duration and peak time were not altered at 0.001–0.01 μM (Fig. 6*C* and *D*). Amplitude and frequency effects were not reversed after a 3 h washout.

To test whether single DAMGO doses elicited similar responses, DAMGO was applied at either 0.01 μM ($n = 4$)

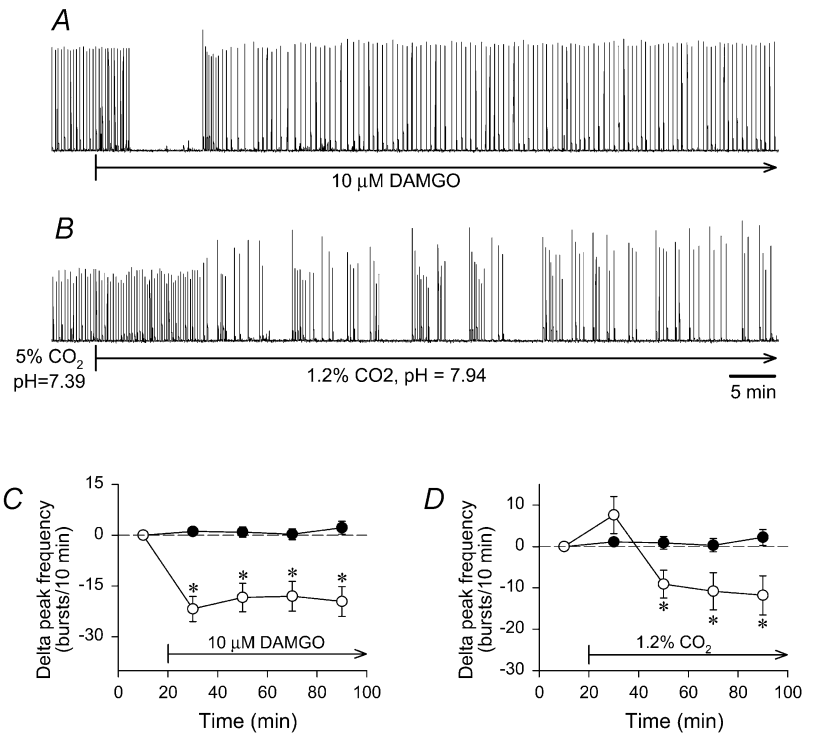

Figure 7. Strychnine-bicuculline rhythm altered by μ-opioid receptor activation and low P_{CO_2}

Brainstems were exposed to bicuculline and strychnine (50 μM each) for 1.5–2.0 h to establish a stable bicuculline–strychnine rhythm before DAMGO or low P_{CO_2} application. *A* and *B*, traces of integrated hypoglossal nerve activity produced during synaptic inhibition blockade by individual brainstems are shown. *A*, DAMGO (10 μM) application abolished rhythmic activity for 8.4 min, and decreased frequency by 19 ± 4 bursts (10 min)$^{-1}$ for the next 60 min. *B*, switching from standard solution containing bicuculline and strychnine (5 % CO_2; pH 7.39) to a similar solution bubbled with 1.2 % CO_2 (pH 7.94) decreased frequency by 33.7 ± 1.2 bursts (10 min)$^{-1}$ within 10 min. For both *C* and *D*, the frequency of the steady-state bicuculline–strychnine rhythm in control brainstems (●; $n = 12$) was 17 ± 2 bursts (10 min)$^{-1}$ at the zero time point, and remained within 17.4–18.5 bursts (10 min)$^{-1}$ for the next 80 min. All data were averaged in 20 min bins. *C*, continuous DAMGO application (10 μM, 80 min) reduced the steady-state bicuculline–strychnine frequency of 22.1 ± 2.4 bursts (10 min)$^{-1}$ by 19.4 ± 0.8 bursts (10 min)$^{-1}$ during 80 min application (○; $n = 8$). *D*, switching from 5 % to 1.2 % CO_2 (80 min) increased the steady-state bicuculline–strychnine frequency of 21.5 ± 1.8 bursts (10 min)$^{-1}$ at the zero time point by 7.6 ± 4.5 bursts (10 min)$^{-1}$ during the first 20 min before causing a decrease of 10.5 ± 0.8 bursts (10 min)$^{-1}$ during the next 60 min (○; $n = 8$). *$P < 0.05$ compared to the first 20 min for delta peak frequencies.

or 0.1 μM (n = 4) after recording baseline data. At 25–45 min during DAMGO application, burst frequency decreased from 7.0 ± 1.7 to 3.4 ± 3.9 bursts (10 min)$^{-1}$ for 0.01 μM, and from 4.3 ± 1.7 to zero bursts (10 min)$^{-1}$ for 0.1 μM. These frequencies were nearly identical to the frequency data points at 0.01 and 0.1 μM in Fig. 6*B*. Burst amplitude, duration and time-to-peak were relatively unaltered (data not shown). Thus, single DAMGO doses altered respiratory rhythm in a manner similar to cumulative doses.

In brainstems (n = 8) expressing the bicuculline–strychnine rhythm, the steady-state frequency was 22.1 ± 2.4 bursts (10 min)$^{-1}$ during a 20 min baseline period. DAMGO (10 μM) significantly reduced frequency by 19.4 ± 0.8 bursts (10 min)$^{-1}$ during the 80 min application (Fig. 7*A–C*). In all brainstems, DAMGO stopped rhythmic activity for 9.4 ± 2.8 min (range 4.9–28.4 min) before activity resumed. Amplitude was unaltered by DAMGO as bursts were 6 ± 5 % larger (P > 0.05) after 60 min of DAMGO application.

CO_2/pH sensitivity. In brainstems (n = 8) expressing the bicuculline–strychnine rhythm with the superfusate equilibrated with 5 % CO_2 (pH = 7.38 ± 0.01), the steady-state frequency was 21.5 ± 1.8 bursts (10 min)$^{-1}$. Switching to an identical solution equilibrated with 1.2 % CO_2 (pH 7.92 ± 0.01) increased burst frequency by 7.6 ± 4.5 bursts (10 min)$^{-1}$ (P > 0.05) during the first 20 min period. During the next 60 min, however, frequency was

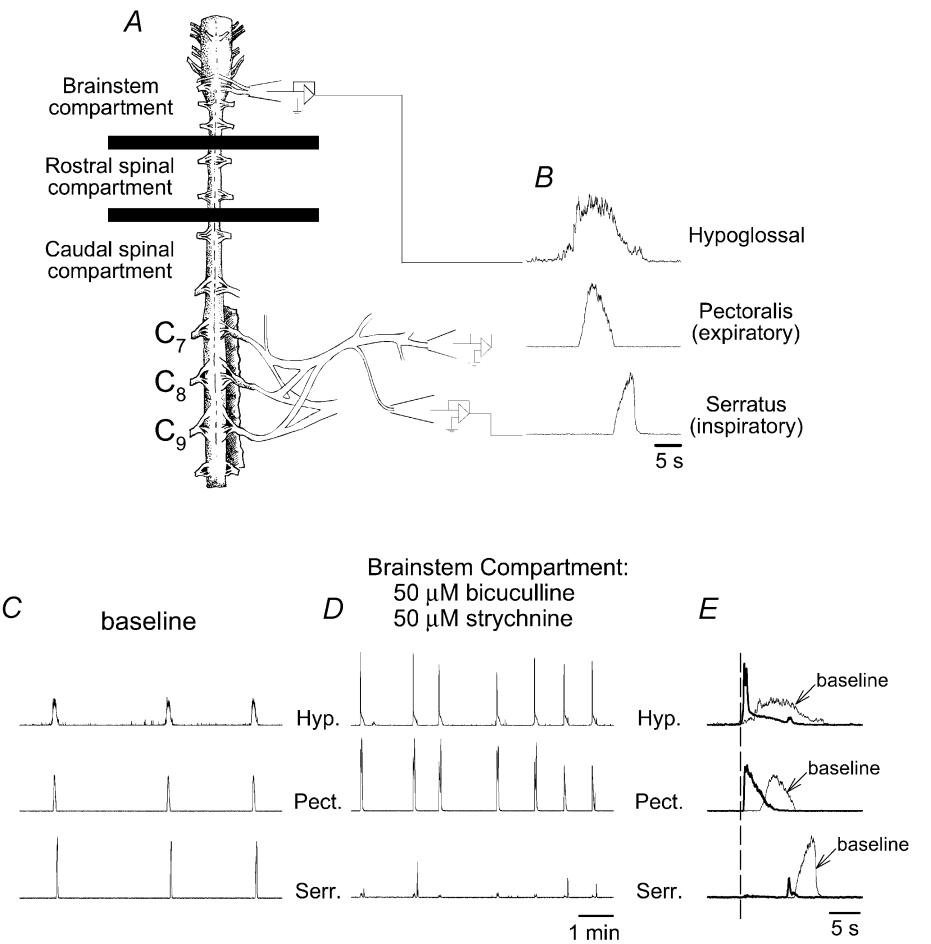

Figure 8. Bicuculline–strychnine rhythm drives expiratory, but not inspiratory, spinal motoneurons

A, schematic drawing of a turtle brainstem–spinal cord preparation with the chamber partitioned into brainstem, rostral spinal, and caudal spinal compartments. *B*, suction electrodes attached to hypoglossal, pectoralis (expiratory), and serratus (inspiratory) nerves record bursts of respiratory activity. Traces of integrated respiratory activity on the three nerves are shown while the brainstem compartment was bathed with control solution (*C*), and with bicuculline and strychnine (50 μM each) (*D*). *E*, individual bursts from baseline recordings (thin lines labelled as 'baseline' with arrows) are superimposed onto bursts recorded during bicuculline–strychnine brainstem application (thick lines). All bursts were aligned with respect to the onset of hypoglossal activity (vertical dashed line). The sample tracings show that hypoglossal and pectoralis amplitudes were increased with the peak time occurring near the onset of activity, whereas serratus activity was nearly abolished. Hyp., hypoglossal; Pect., pectoralis; Serr., serratus.

significantly decreased by an average of 10.5 ± 0.8 bursts (10 min)$^{-1}$ (Fig. 7*B–D*). Amplitude was unaltered as bursts were 12 ± 8 % larger ($P > 0.05$) after 60 min of exposure to the lower P_{CO_2}.

Bicuculline–strychnine rhythm produces spinal expiratory activity

Semi-aquatic turtles breathe by moving their pectoral (neck and forelimbs) and pelvic (tail and hindlimbs) girdles inward and outward to generate positive (expiratory) and negative (inspiratory) lung pressures (Gans & Hughes, 1967; Gaunt & Gans, 1967). To move the pectoral girdle, respiratory rhythm in the brainstem is transmitted to pectoralis (expiratory) and serratus (inspiratory) cervical spinal motoneurons (Gans & Hughes, 1967; Takeda *et al.* 1986). An *in vitro* turtle brainstem–spinal cord spontaneously produces respiratory motor output very similar to that produced by intact turtles (Johnson & Mitchell, 1998). Expiratory activity in pectoralis motoneurons occurs with an incrementing–decrementing pattern shortly after hypoglossal burst onset, while

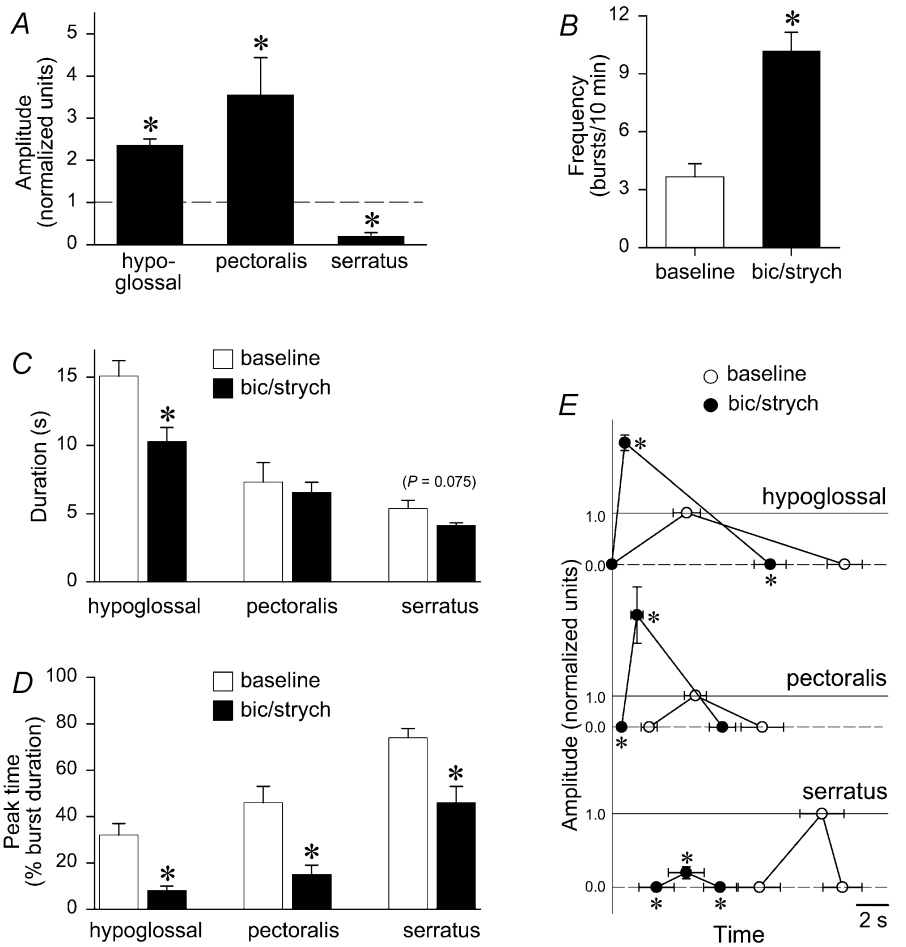

Figure 9. Characteristics of rhythm during brainstem $GABA_A$ and glycine receptor blockade

Group data for brainstem–spinal cord preparations ($n = 6$) under baseline conditions, and following blockade of $GABA_A$ and glycine receptors in the brainstem. All data were averaged in 20 min bins. *A*, hypoglossal and pectoralis burst amplitude increased by 140 % and 260 %, respectively ($P < 0.05$), whereas serratus burst amplitude decreased by 80 % ($P < 0.05$). *B*, frequency increased significantly by nearly 7 bursts (10 min)$^{-1}$. *C*, duration decreased in all three nerves, but a significant decrease was observed only in hypoglossal bursts. Open bars indicate baseline data; black bars indicate data during blockade of brainstem $GABA_A$ and glycine receptors. *D*, peak time significantly shifted from the middle to the beginning of the burst in hypoglossal and pectoralis nerves, whereas peak time significantly shifted from near the end of the burst to the middle of the burst for serratus nerves. *E*, burst onset, peak time, burst amplitude relative to baseline (horizontal dashed lines), and burst termination are graphed for baseline (○) and blockade of brainstem $GABA_A$ and glycine receptors (●) for hypoglossal, pectoralis, and serratus. All timing data are graphed with respect to the onset of hypoglossal activity. Baseline amplitude is set at 1.0 arbitrary units (horizontal continuous lines); amplitude at burst onset and burst termination is set at zero (horizontal dashed lines). * Significant differences with respect to baseline in terms of timing only; significant amplitude differences have already been indicated in Fig. 9*A*.

inspiratory activity in serratus motoneurons increases in a ramp-like pattern before abruptly terminating (Fig. 8).

To determine how $GABA_A$ and glycine receptor blockade in the brainstem alters respiratory spinal motor output, bicuculline and strychnine (50 μM each) were applied to the brainstem compartment of brainstem–spinal cord preparations ($n = 6$; Fig. 8*A*). Frequency increased from 3.7 to 10.2 bursts $(10\ min)^{-1}$ ($P < 0.05$; Figs 8*D* and 9*B*). Hypoglossal bursts increased amplitude by 140 % ($P < 0.05$; Figs 8*E* and 9*A*), decreased duration by 4.8 s ($P < 0.05$; Figs 8*E* and 9*C*), and decreased peak time from 32 % to 8 % ($P < 0.05$; Figs 8*E* and 9*D*). Spinal expiratory activity in pectoralis increased amplitude by 260 % ($P < 0.05$; Figs 8*E* and 9*A*), was not altered in duration (Fig. 9*C*), and decreased peak time from 46 % to 15 % ($P < 0.05$; Figs 8*E* and 9*D*). Spinal inspiratory activity in serratus was nearly abolished because amplitude decreased by 80 % ($P < 0.05$; Figs 8*E* and 9*A*). Duration was not altered ($P = 0.075$; Fig. 9*C*) and peak time decreased from 74 % to 46 % ($P < 0.05$; Figs 8*E* and 9*D*).

A composite graph illustrates timing and amplitude changes in hypoglossal, pectoralis, and serratus nerve discharges before and after application of bicuculline–strychnine solution to the brainstem (Fig. 9*E*). During synaptic inhibition blockade, hypoglossal burst amplitude was larger, duration was shorter and peak time shifted from the middle to the onset of activity. Similarly, pectoralis burst amplitude was larger, duration was not significantly shorter, and peak time was shifted from the middle to the onset of activity. In contrast, serratus burst amplitude was much smaller, duration was not significantly shorter, and the characteristic slow-incrementing pattern (Fig. 8*B*) was abolished. The phasic pattern of pectoralis and serratus activity was also altered. In controls, the onset of serratus (inspiratory) activity always follows, or is closely coincident with, the end of pectoralis (expiratory) activity (Figs 8*B*, 8*E* and 9*E*; see also Johnson & Mitchell, 1998). Following synaptic inhibition blockade, serratus activity occurred during the latter half of hypoglossal and pectoralis discharge, but peak serratus activity still occurred after peak pectoralis activity (Fig. 9*E*).

DISCUSSION

This study is the first to show that rhythmic activity persists in an adult vertebrate *in vitro* brainstem preparation during both $GABA_A$ and glycine receptor blockade. The bicuculline–strychnine rhythm appears to involve respiratory-related neurons because μ-opioid receptor activation and low P_{CO_2} reduced rhythm frequency. Although these data do not decisively favour either network or pacemaker models for rhythmogenesis, they show that an adult vertebrate respiratory rhythm generator has the capacity to exhibit properties consistent with a pacemaker-driven network. These data are also consistent with our working hypothesis that chemosensitive expiratory neurons with pacemaker properties contribute to respiratory rhythm generation in turtles.

Synaptic inhibition blockade

Glycine receptors. Glycine receptor blockade with strychnine increases respiratory frequency in neonatal and mature vertebrate preparations (Schmid *et al.* 1991; Hayashi & Lipski, 1992; Galante *et al.* 1996; Ramirez *et al.* 1996; Kimura *et al.* 1997; Shao & Feldman, 1997; Bou-Flores & Berger, 2001; Büsselberg *et al.* 2001). In turtle brainstems, however, low concentrations of strychnine (0.01–1.0 μM) did not alter hypoglossal activity; increased hypoglossal frequency and burst amplitude were observed only at higher concentrations (10–50 μM). However, strychnine effects at 10–50 μM may have been due to $GABA_A$ receptor blockade, since strychnine is reported to be a $GABA_A$ receptor antagonist at concentrations greater than 1.0 μM (Jonas *et al.* 1998). Although further experiments are required to determine whether strychnine crossed over to block $GABA_A$ receptors in turtles, glycine receptors may not play a prominent role in regulating turtle respiratory frequency.

Strychnine did alter burst duration in a dose-dependent manner in turtle brainstems, similarly to its effects on other vertebrate preparations (Schmid *et al.* 1991; Hayashi & Lipski, 1992; Paton & Richter, 1995; Galante *et al.* 1996; Ramirez *et al.* 1996, 1997; Kimura *et al.* 1997; Shao & Feldman, 1997; Lieske *et al.* 2000; Büsselberg *et al.* 2001), and 10–50 μM strychnine tended to transform hypoglossal bursts into a rapid onset–decrementing pattern , as seen in *in situ* frog brainstems (Kimura *et al.* 1997). Thus, glycine receptors in turtle brainstems appear primarily to regulate respiratory burst shape (Lieske *et al.* 2000).

GABA receptors. Bicuculline increased respiratory burst frequency and amplitude in turtle brainstems, similar to results obtained using *in vitro* neonatal rodent preparations (Smith & Feldman, 1987; Paton & Richter, 1995; Shao & Feldman, 1997, but see Bou-Flores & Berger, 2001) and perfused adult rats (Hayashi & Lipski, 1992). In tadpole brainstems, however, bicuculline increased frequency with variable amplitude effects (Galante *et al.* 1996). Burst duration was decreased by bicuculline in turtle brainstems and murine medullary slices (more than 15 days old; Paton & Richter, 1995), but not in perfused adult rats (Hayashi & Lipski, 1992). Although there is some variability in $GABA_A$-dependent effects, which may be due to differences between motoneuron pools (e.g. hypoglossal *vs.* phrenic *vs.* trigeminal pools) or of species or age, most data indicate that $GABA_A$ receptors regulate respiration. In contrast, $GABA_B$ receptors do not appear to play a necessary role in respiratory rhythm generation since $GABA_B$ receptor blockade does not alter respiratory activity in turtle

brainstems (Fig. 4) or neonatal rat brainstem–spinal cord preparations (Feldman & Smith, 1989; Brockhaus & Ballanyi, 1998).

Combined $GABA_A$ and glycine receptor blockade. Combined $GABA_A$ and glycine receptor blockade in turtle brainstems produced robust (albeit altered) rhythmic motor activity in hypoglossal and pectoralis (expiratory) nerves. To our knowledge, this is the first demonstration of rhythmic motor activity persisting during blockade of synaptic inhibition in an adult vertebrate. Previously, rhythmic activity was produced under these conditions only in *in vitro* neonatal and juvenile rodent preparations (Smith & Feldman, 1987; Feldman *et al.* 1989, 1990; Shao & Feldman, 1997; Brockhaus & Ballanyi, 1998; Bou-Flores & Berger, 2001; Johnson *et al.* 2001*a*). The tadpole brainstem preparation is particularly interesting because it contains gill and lung rhythmic motor networks (Torgerson *et al.* 2001; Wilson *et al.* 2002), which differentially respond to synaptic inhibition blockade. Since synaptic inhibition blockade abolishes fictive gill ventilation while fictive lung ventilation persists (Galante *et al.* 1996), it is hypothesized that these two highly integrated respiratory motor networks use distinct mechanisms (i.e. are network- *vs.* pacemaker-driven) to generate rhythmic motor output (reviewed in Gdovin *et al.* 1999). In contrast, synaptic inhibition blockade in intact adult mammalian preparations is reported to completely disrupt respiratory rhythm and may induce seizure-like activity (Schmid *et al.* 1991; Hayashi & Lipski, 1992; Paton & Richter, 1995; Pierrefiche *et al.* 1998).

One caveat is that synaptic inhibition within the turtle respiratory rhythm generator may not have been completely abolished during bicuculline–strychnine application. At 50 μM concentrations, virtually all mammalian $GABA_A$ and glycine receptors are blocked by bicuculline and strychnine, respectively (Jonas *et al.* 1998). It is not known, however, whether $GABA_A$ and glycine receptor-induced currents in turtle central neurons are likewise blocked at these concentrations. Significant alterations in $GABA_A$ and glycine receptor-dependent responses in turtle neurons are reported for bath application of 3.5–100 μM bicuculline (Larson-Prior & Slater, 1988; Akopian *et al.* 1998; Russo *et al.* 1998; Mancilla & Ulinksi, 2001) and 5–20 μM strychnine (Currie & Lee, 1997; Russo *et al.* 1998). Thus, this question needs to be addressed via intracellular recordings of brainstem respiratory neurons. In addition, other mechanisms of synaptic inhibition may have still remained functional during bicuculline–strychnine application, such as K^+ conductance activation, synaptic blockade via presynaptic depolarization, or shunting of postsynaptic currents near the axon hillock or at dendritic branches (see discussion in Feldman *et al.* 1989). There is, however, very little experimental evidence that any of these mechanisms contribute to respiratory rhythm generation.

Which model best explains turtle respiratory rhythm generation?

Current models for respiratory rhythm generation are controversial. The data in this study are not sufficient to rule out any particular model, or make one model more attractive than the others.

Pacemaker-driven models. In turtle brainstems, the persistence of rhythmic activity during synaptic inhibition blockade suggests that synaptic inhibition is not required for respiratory rhythm generation. The chemosensitive, μ-opioid-sensitive bicuculline–strychnine rhythm is consistent with the hypothesis that respiratory neurons involved in rhythm generation have pacemaker properties that are revealed during synaptic inhibition blockade, as proposed by the hybrid pacemaker-network model (Smith *et al.* 1995; Butera *et al.* 1999*a*, *b*; Koshiya & Smith, 1999; Smith *et al.* 2000). In neonatal rodents, the pacemaker neurons thought to underlie rhythm generation are pre-inspiratory neurons, i.e. neurons hypothesized to initiate bursts of activity within the respiratory network (Smith *et al.* 1991, 1995; Butera *et al.* 1999*a*, *b*; Koshiya & Smith, 1999; Smith *et al.* 2000). Our data suggest that expiratory neurons, which are active at the onset of the turtle respiratory cycle (McCutcheon, 1943; Gans & Hughes, 1967; Gaunt & Gans, 1967; Milsom & Jones, 1980; Silver & Jackson, 1985; Takeda *et al.* 1986), are pacemaker neurons because rhythmic activity during synaptic inhibition blockade was expressed in spinal expiratory nerves in the brainstem–spinal cord preparations (Figs 8 and 9).

The role of pacemaker properties in respiratory rhythm generation, however, remains controversial. Some investigators suggest that respiratory-related pacemaker neurons synchronize or amplify recurrent excitation within the network, rather than play a major role in generating rhythmicity (Ramirez & Richter, 1996; Richter & Spyer, 2001; Del Negro *et al.* 2002). Alternatively, pacemaker neurons may provide a fail-safe mechanism for maintaining breathing during certain physiological and pathophysiological conditions whereby synaptic transmission is decreased, such as extreme hypoxia (McCrimmon *et al.* 2000). Another interpretation is that synaptic inhibition blockade causes changes in respiratory network function that allow respiratory-related neurons to express pacemaker properties that are not ordinarily expressed *in vivo*. From this point of view, pacemaker properties in respiratory neurons might be an artifact of *in vitro* conditions and synaptic inhibition blockade. Although determining the role of pacemaker properties in rhythm generation remains a technically challenging problem, the turtle brainstem preparation provides the opportunity to test whether expiratory neurons (that may belong to the respiratory rhythm generator of an adult vertebrate) have pacemaker properties, and whether these neurons are chemosensitive and μ-opioid-sensitive.

Our data are also consistent with the group-pacemaker model (Rekling & Feldman, 1998; Del Negro *et al.* 2002), which proposes that excitatory synaptic inputs within a network of highly interconnected (expiratory) neurons gradually increase until all neurons synchronously fire action potential bursts (pacemaker neurons are not required). This model is supported by evidence that turtle brainstem expiratory neurons gradually depolarize due to increasing excitatory synaptic inputs prior to firing action potentials during expiration (Takeda *et al.* 1986). The source of excitatory synaptic inputs may be located elsewhere in the brainstem (as proposed by Takeda *et al.* 1986), or by other expiratory neurons as proposed by the group-pacemaker model. Further experiments will be required to directly test predictions of the group-pacemaker model.

Network models and the 'switching' hypothesis. Although synaptic inhibition may not be necessary for turtle respiratory rhythm generation, network models cannot be ruled out because the respiratory network may have been switched from a network-based system to a pacemaker-driven system during synaptic inhibition blockade, or in a manner suggested by the 'switching' hypothesis (Rybak *et al.* 2001; see also Büsselberg *et al.* 2001). The switching hypothesis suggests that increased extracellular $[K^+]$ and decreased phasic synaptic inhibition 'release' pacemaker neurons from inhibitory synaptic mechanisms that regulate neuronal excitability. The released chemosensitive pacemaker neurons then burst freely and force downstream respiratory neurons to rhythmically fire action potentials. The switching hypothesis is congruent with network models because no respiratory rhythm-generating neurons are proposed to have pacemaker properties. In other words, the chemosensitive pacemaker neurons are considered to be outside the normal respiratory rhythm-generating network, although this assumption has little experimental verification. Nevertheless, our data are consistent with the switching hypothesis because turtle brainstems produced a chemosensitive rhythm during synaptic inhibition blockade. It remains unclear if rhythmic neurons are respiratory rhythm-generating neurons, or central chemosensory neurons normally separate from the rhythm generator. Thus, our data do not provide evidence for or against the switching hypothesis.

In summary, following synaptic inhibition blockade, the turtle respiratory network is still able to produce a rhythm that is sensitive to characteristic respiratory stimuli. This is consistent with several models of vertebrate respiratory rhythm generation that incorporate respiratory pacemaker neurons. However, in this case, the rhythm is observed in expiratory (rather than inspiratory) motor output, suggesting an expiratory pacemaker. Our data do not allow conclusions regarding the role of pacemaker neurons in normal respiratory rhythm generation; rather they indicate that the system has the potential to operate in a pacemaker-driven manner.

REFERENCES

Akopian, A., Gabriel, R. & Witkovsky, P. (1998). Calcium released from intracellular stores inhibits $GABA_A$-mediated currents in ganglion cells of the turtle retina. *Journal of Neurophysiology* **80**, 1105–1115.

Bou-Flores, C. & Berger, A.J. (2001). Gap junctions and inhibitory synapses modulate inspiratory motoneuron synchronization. *Journal of Neurophysiology* **85**, 1543–1551.

Brockhaus, J. & Ballanyi, K. (1998). Synaptic inhibition in the isolated respiratory network of neonatal rats. *European Journal of Neuroscience* **10**, 3823–3839.

Büsselberg, D., Bischoff, A. M., Paton, J. F. R. & Richter, D. W. (2001). Reorganisation of respiratory network activity after loss of glycinergic inhibition. *Pflügers Archiv* **441**, 444–449.

Butera, R. J., Rinzel, J. & Smith, J. C. (1999*a*). Models of respiratory rhythm generation in the pre-Bötzinger complex. I. Bursting pacemaker neurons. *Journal of Neurophysiology* **81**, 382–397.

Butera, R. J., Rinzel, J. & Smith, J. C. (1999*b*). Models of respiratory rhythm generation in the pre-Bötzinger complex. II. Populations of coupled pacemaker neurons. *Journal of Neurophysiology* **81**, 398–415.

Currie, S. N. & Lee, S. (1997). Glycinergic inhibition contributes to the generation of rostral scratch motor patterns in the turtle spinal cord. *Journal of Neuroscience* **17**, 3323–3333.

Del Negro, C. A., Morgado-Valle, C. & Feldman, J. L. (2002). Respiratory rhythm: an emergent network property? *Neuron* **34**, 821–830.

Douse, M. A. & Mitchell, G. S. (1990). Episodic respiratory related discharge in turtle cranial motoneurons: *in vivo* and *in vitro* studies. *Brain Research* **536**, 297–300.

Duffin, J., Ezure, K. & Lipski, J. (1995). Breathing rhythm generation: focus on the rostral ventrolateral medulla. *News in Physiological Science* **10**, 133–140.

Feldman, J. L. & Cleland, C. L. (1982). Possible roles of pacemaker neurons in mammalian respiratory rhythmogenesis. In *Cellular Pacemakers,* ed. Carpenter, D.O., pp. 101–119. John Wiley and Sons, NY, USA.

Feldman, J. L. & Smith, J. C. (1989).Cellular mechanisms underlying modulation of breathing patterns in mammals. *Annals of the New York Academy of Science* **563**, 114–130.

Feldman, J. L., Smith, J. C., Ellenberger, H. H., Connelly, C. A., Liu, G., Greer, J. J., Lindsay, A. D. & Otto, M. R. (1990). Neurogenesis of respiratory rhythm and pattern: emerging concepts. *American Journal of Physiology* **28**, R879–886.

Feldman, J. L., Smith, J. C., Ellenberger, H. H., Fournier, M. & Connelly, C. A. (1989). Breathing in mammals: rhythm and pattern. In *Neuronal and Cellular Oscillators,* ed. Jacklet, J. W., pp. 435–456. Marcel Dekker, NY, USA.

Funk, G. D. & Feldman, J. L. (1995). Generation of respiratory rhythm and pattern in mammals: insights from developmental studies. *Current Opinion in Neurobiology* **5**, 778–785.

Galante, R. J., Kubin, L., Fishman, A. P. & Pack, A. I. (1996). Role of chloride-mediated inhibition in respiratory rhythmogenesis in an in vitro brainstem of a tadpole, *Rana catesbeiana*. *Journal of Physiology* **492**, 545–558.

Gans, C. & Hughes, G. M. (1967). The mechanism of lung ventilation in the tortoise *Testudo graeca linné*. *Journal of Experimental Biology* **47**, 1–20.

Gaunt, A. S. & Gans, C. (1967) Mechanics of respiration in the snapping turtle, *Chelydra serpentina* (Linné). *Journal of Morphology* **128**, 195–226.

Gdovin, M. J., Torgerson, C. S. & Remmers, J. E. (1999). The fictively breathing tadpole brainstem preparation as a model for the development of respiratory pattern generation and central chemoreception. *Comparative Biochemistry and Physiology* A **124**, 275–286.

Getting, P.A. (1988). Comparative analysis of invertebrate central pattern generators. In *Neural Control of Rhythmic Movements in Vertebrates*, ed. Cohen, A. H., Rossignol, S. & Grillner, S., pp. 101–127. John Wiley and Sons, NY, USA.

Gray, P. A., Janczewski, W. A., Mellen, N., McCrimmon, D. R. & Feldman, J. L. (2001). Normal breathing requires pre-Bötzinger Complex neurokinin-1 receptor-expressing neurons. *Nature Neuroscience* **4**, 927–930.

Hayashi, F. & Lipski, J. (1992). The role of inhibitory amino acids in control of respiratory motor output in an arterially perfused rat. *Respiration Physiology* **89**, 47–63.

Johnson, S. M., Johnson, R. A. & Mitchell, G. S. (1998). Hypoxia, temperature and pH/CO_2 effects on respiratory discharge from a turtle brain stem preparation. *Journal of Applied Physiology* **84**, 649–660.

Johnson, S. M., Koshiya, N. & Smith, J. C. (2001*a*). Isolation of the kernel for respiratory rhythm generation in a novel preparation: the pre-Bötzinger complex 'island'. *Journal of Neurophysiology* **85**, 1772–1776.

Johnson, S. M. & Mitchell, G. S. (1998). NMDA-mediated bulbospinal respiratory drive is pH/P_{CO_2}-insensitive in turtle brainstem-spinal cord preparation. *Respiration Physiology* **113**, 201–212.

Johnson, S. M., Smith, J. C., Funk, G. D. & Feldman, J. L. (1994). Pacemaker behavior of respiratory neurons in medullary slices from neonatal rat. *Journal of Neurophysiology* **72**, 2598–2608.

Johnson, S. M., Wilkerson, J. E. R., Henderson, D. R. & Wenninger, M. R. (2001*b*). Role of synaptic inhibition in respiratory rhythm generation in turtle brainstems *in vitro*. *Society for Neuroscience Abstracts* **243**,4.

Jonas, P., Bischofberger, J. & Sandkühler, J. (1998). Corelease of two fast neurotransmitters at a central synapse. *Science* **281**, 419–424.

Kimura, N., Perry, S. F. & Remmers, J. E. (1997). Strychnine eliminates reciprocation and augmentation of respiratory bursts of the *in vitro* frog brainstem. *Neuroscience Letters* **225**, 9–12.

Koshiya, N. & Smith, J. C. (1999). Neuronal pacemaker for breathing visualized *in vitro*. *Nature* **400**, 360–363.

Larson-Prior, L. J. & Slater, N. T. (1988). GABA ergic inhibition and epileptiform discharges in the turtle hippocampus *in vitro*. *Brain Research* **460**, 369–375.

Lieske, S. P., Thoby-Brisson, M., Telgkamp, P. & Ramirez, J. M. (2000). Reconfiguration of the neural network controlling multiple breathing patterns: eupnea, sighs and gasps. *Nature Neuroscience* **3**, 600–607.

McCrimmon, D. R., Ramirez, J. M., Alford, S. & Zuperku, E. J. (2000). Unraveling the mechanism for respiratory rhythm generation. *BioEssays* **22**, 6–9.

McCutcheon, F. H. (1943). The respiratory mechanism in turtles. *Physiological Zoology* **3**, 255–269.

Mancilla, J. G. & Ulinkski, P. S. (2001). Role of $GABA_A$-mediated inhibition in controlling the responses of regular spiking cells in turtle visual cortex. *Visual Neuroscience* **18**, 9–24.

Milsom, W. K. & Jones, D. R. (1980). The role of vagal afferent information and hypercapnia in control of the breathing pattern in chelonia. *Journal of Experimental Biology* **87**, 53–63.

Paton, J. F. R., Ramirez, J. M. & Richter, D. W. (1994). Mechanisms of respiratory rhythm generation change profoundly during early life in mice and rats. *Neuroscience Letters* **170**, 167–270.

Paton, J. F .R. & Richter, D. W. (1995). Role of fast inhibitory synaptic mechanisms in respiratory rhythm generation in the maturing mouse. *Journal of Physiology* **484**, 505–521.

Pierrefiche, O., Schwarzacher, S. W., Bischoff, A. M. & Richter, D. W. (1998). Blockade of synaptic inhibition within the pre-Bötzinger complex in the cat suppresses respiratory rhythm generation *in vivo*. *Journal of Physiology* **509**, 245–254.

Ramirez, J. M., Quellmalz, U. J. A. & Richter, D. W. (1996). Postnatal changes in the mammalian respiratory network as revealed by the transverse brainstem slice of mice. *Journal of Physiology* **491**, 799–812.

Ramirez, J. M. & Richter, D. W. (1996). The neuronal mechanisms of respiratory rhythm generation. *Current Opinion in Neurobiology* **6**, 817–825.

Ramirez, J. M., Schwarzacher, S. W., Pierrefiche, O., Olivera, B. M. & Richter, D. W. (1998). Selective lesioning of the cat pre-Bötzinger complex *in vivo* eliminates breathing but not gasping. *Journal of Physiology* **507**, 895–907.

Ramirez, J. M., Telgkamp, P., Elsen, F. P., Quellmalz, U. J. A. & Richter, D. W. (1997). Respiratory rhythm generation in mammals: synaptic and membrane properties. *Respiration Physiology* **110**, 71–85.

Rekling, J. C., Champagnat, J. & Denavit-Saubie, M. (1996). Electroresponsive properties and membrane potential trajectories of three types of inspiratory neurons in the newborn mouse brain stem *in vitro*. *Journal of Neurophysiology* **75**, 795–810.

Rekling, J. C. & Feldman, J. L. (1998). Pre-Bötzinger complex and pacemaker neurons: hypothesized site and kernel for respiratory rhythm generation. *Annual Review of Physiology* **60**, 385–405.

Richter, D. W., Ballanyi, K. & Ramirez, J. M. (1997). Respiratory rhythm generation. In *Neural Control of the Respiratory Muscles*, ed. Miller, A. D., Bianchi, A. L. & Bishop, B. P., pp. 119–130. CRC Press, USA.

Richter, D. W., Ballanyi, K. & Schwarzacher, S. (1992). Mechanisms of respiratory rhythm generation. *Current Opinion in Neurobiology* **2**, 788–793.

Richter, D. W. & Spyer, K. M. (2001). Studying rhythmogenesis of breathing: comparison of *in vivo* and *in vitro* models. *Trends in Neurosciences* **8**, 464–472.

Russo, R. E., Nagy, F. & Hounsgaard, J. (1998). Inhibitory control of plateau properties in dorsal horn neurones in the turtle spinal cord *in vitro*. *Journal of Physiology* **506**, 795–808.

Rybak, I. A., Paton, J. F .R. & Schwaber, J. S. (1997). Modeling neural mechanisms for genesis of respiratory rhythm and pattern. II. Network models of the central respiratory pattern generator. *Journal of Neurophysiology* **77**, 2007–2026.

Rybak, I. A., St John, W. M. & Paton, J. F. R. (2001). Models of neuronal bursting behavior: implications for *in vivo* versus *in vitro* respiratory rhythmogenesis. In *Frontiers in Modeling and Control of Breathing: Integration at Molecular, Cellular and Systems Levels*, ed. Poon, C. S., pp. 159–164. Klewer Press, NY, USA.

Schmid, K., Böhmer, G. & Gebauer, K. (1991). Glycine receptor-mediated fast synaptic inhibition in the brainstem respiratory system. *Respiration Physiology* **84**, 351–361.

Shao, X. M. & Feldman, J. L. (1997). Respiratory rhythm generation and synaptic inhibition of expiratory neurons in the pre-Bötzinger complex: differential roles of glycinergic and GABAergic neural transmission. *Journal of Neurophysiology* **77**, 1853–1860.

Silver, R. B. & Jackson, D. C. (1985). Ventilatory and acid–base responses to long-term hypercapnia in the freshwater turtle, *Chrysemys picta bellii*. *Journal of Experimental Biology* **114**, 661–672.

Smith, J. C., Butera, R. J., Koshiya, N., Del Negro, C., Wilson, C. G. & Johnson, S. M. (2000). Respiratory rhythm generation in neonatal and adult mammals: the hybrid pacemaker-network model. *Respiration Physiology* **122**, 131–147.

Smith, J. C., Ellenberger, H. H., Ballanyi, K., Richter, D. W. & Feldman, J. L. (1991). Pre-Bötzinger complex: a brainstem region that may generate respiratory rhythm in mammals. *Science* **254**, 726–729.

Smith, J. C. & Feldman, J. L. (1987). Central respiratory pattern generation studied in an *in vitro* mammalian brainstem–spinal cord preparation. In *Respiratory Muscles and Their Neuromotor Control,* ed. Seick, G., Gandevia, S. C. & Cameron, W. E., pp. 27–36. AR Liss, NY, USA.

Smith, J. C., Funk, G. D., Johnson, S. M. & Feldman, J. L. (1995). Cellular and synaptic mechanisms generating respiratory rhythm: insights from *in vitro* and computational studies. In *Ventral Brainstem Mechanisms and Control of Respiration and Blood Pressure,* ed. Trouth, C. O., Millis, R., Kiwull-Schone, H. & Schlaefke, M., pp. 463–496. Marcel Dekker, NY, USA.

Takeda, R., Remmers, J. E., Baker, J. P., Madden, K. P. & Farber, J. P. (1986). Postsynaptic potentials of bulbar respiratory neurons of the turtle. *Respiration Physiology* **64**, 149–160.

Thoby-Brisson, M. & Ramirez, J. M. (2000). Role of inspiratory pacemaker neurons in mediating the hypoxic response of the respiratory network *in vitro*. *Journal of Neuroscience* **20**, 5858–5866.

Thoby-Brisson, M. & Ramirez, J. M. (2001). Identification of two types of inspiratory pacemaker neurons in the isolated respiratory neural network of mice. *Journal of Neurophysiology* **86**, 104–112.

Torgerson, C. S., Gdovin, M. J. & Remmers, J. E. (2001). Sites of respiratory rhythmogenesis during development in the tadpole. *American Journal of Physiology – Regulatory, Integrative and Comparative Physiology* **280**, R913–920.

Wilson, R. J. A., Vasilakos, K., Harris, M. B., Straus, C. & Remmers, J. E. (2002). Evidence that ventilatory rhythmogenesis in the frog involves two distinct neuronal oscillators. *Journal of Physiology*, **540**, 557–570.

Acknowledgements

This work was supported by National Heart, Lung and Blood Institute Grants HL-60028 and HL-53319. J.E.R.W. is supported by a National Science Foundation predoctoral fellowship.